Colloids and Surfaces B: Biointerfaces 161 (2018) 670–676

Contents lists available at ScienceDirect

Colloids and Surfaces B: Biointerfaces

journal homepage: www.elsevier.com/locate/colsurfb

Full length article

Controlling insulin release from reverse hexagonal (H_{II}) liquid crystalline mesophase by enzymatic lipolysis

Tehila Mishraki-Berkowitz [a,1], Guy Cohen [b], Abraham Aserin [a], Nissim Garti [a,*]

[a] The Ratner Chair in Chemistry, Casali Institute of Applied Chemistry, The Institute of Chemistry, The Hebrew University of Jerusalem, Edmond J. Safra Campus, Jerusalem 9190401, Israel
[b] Skin Research Institute, Dead-Sea & Arava Science Center, Ein Gedi, Israel

ARTICLE INFO

Article history:
Received 27 June 2017
Received in revised form 29 October 2017
Accepted 11 November 2017
Available online 12 November 2017

Keywords:
Reverse hexagonal liquid crystal (H_{II} mesophase)
Thermomyces lanuginosa lipase (TLL)
Insulin
Drug release
Phosphatidylcholine (PC)
Monoolein

ABSTRACT

In the present study we aimed to control insulin release from the reverse hexagonal (H_{II}) mesophase using *Thermomyces lanuginosa* lipase (TLL) in the environment (outer TLL) or within the H_{II} cylinders (inner TLL). Two insulin-loaded systems differing by the presence (or absence) of phosphatidylcholine (PC) were examined.

In general, incorporation of PC into the H_{II} interface (without TLL) increased insulin release, as a more cooperative system was formed.

Addition of TLL to the systems' environments resulted in lipolysis of the H_{II} structure. In the absence of PC, the lipolysis was more dominant and led to a significant increase in insulin release (50% after 8 h). However, the presence of PC stabilized the interface, hindering the lipolysis, and therefore no impact on the release profile was detected during the first 8 h.

Entrapment of TLL within the H_{II} cylinders (with and without PC) drastically increased insulin release in both systems up to 100%. In the presence of PC insulin released faster and the structure was more stable.

Consequently, the presence of lipases (inner or outer) both enhanced the destruction of the carrier, and provided sustained release of the entrapped insulin.

1. Introduction

Reverse hexagonal (H_{II}) lyotropic liquid crystals (LLCs) are self-assembled, long, and dense micelles, arranged in a two-dimensional array. Each of these cylinders is formed by a layer of surfactant molecules, in which the lipophilic moieties point outward and the hydrophilic heads point inward. The cylinders are filled with a hydrophilic solvent, which is usually water [1–3]. Hence, those structures enable the entrapment of lipophilic molecules between the lipid moieties, and water-soluble compounds within the aqueous domains. One of the most studied surfactants that create the LLCs' matrices and in particular the H_{II} mesophase is glycerol monooleate (GMO). This system was shown to have potential applications as a host system for drug delivery [4–7], food applications [8,9], and protein crystallization [5,10–14].

The H_{II} mesophase (containing GMO/water), that commonly assembled at 80 °C and inverts to other structures upon cooling [15], was stabilized at room temperature by the addition of a specific triacylglycerol ester (triglyceride, TAG) [16]. This stabilization enables utilization of the H_{II} system for incorporation of bioactive molecules, and in particular peptides and globular proteins [5,17]. It was shown that the H_{II} carrier improves the conformational stability of the model protein (lysozyme, LSZ) as a function of temperature, pH, and denaturing agent (urea) [18,19]. Furthermore, the H_{II} system enables sustained and controlled release [7,20–22].

Of special interest is the protein insulin, which is a hormone regulating carbohydrate and fat metabolism. Diabetes mellitus is a pathological condition characterized by an absolute or relative lack of insulin resulting in high blood glucose due to the inability to transport the glucose into cells (Type 1–juvenile, Type 2–adult) [23–25]. Hence, exogenous insulin must be administered by daily subcutaneous (s.c.) injection [26,27]. Although the oral route would be preferable, this has not been achievable due to denaturing of the insulin as it travels down the gastrointestinal tract (GIT). Therefore, we have recently focused our research on embedment of insulin into the H_{II} system [28–31], as it was shown that oral insulin can

* Corresponding author.
E-mail address: garti@mail.huji.ac.il (N. Garti).
[1] The results presented in this paper will appear in the Ph.D. dissertation of T.M.-B. in partial fulfillment of the requirements for the Ph.D. degree in Chemistry, The Hebrew University of Jerusalem, Israel.

https://doi.org/10.1016/j.colsurfb.2017.11.031
0927-7765/

be comparable to s.c. insulin with regard to glycemic efficacy and safety [32,33].

Insulin-loading into the H_{II} carrier was found to destabilize the structure [29] and to disorder the interface [28], as insulin was located in the water core and in between the GMO headgroups. Insulin encapsulation enhanced the formation of the α-helix structure, which characterizes a more stable conformation, compared to when it is dissolved in aqueous solution [30]. Addition of the co-surfactant phosphatidylcholine (PC) to the H_{II} system significantly increased insulin's cumulative release [31]. However, a major part of the insulin content still remained "trapped" in the H_{II} matrix. Rupture of the hexagonal structure would enable the release of the "trapped" insulin and control the insulin release rate.

Thermomyces lanuginosa lipase (TLL) was shown to cause lipolysis of the LLCs' structures and to provide structural transitions, as the lipid composition was modified during lipolytic processes [34–36]. Our laboratory's previous study demonstrated that addition of TLL to the H_{II} system disordered and decomposed the hexagonal mesophase, and thereby enhanced the diffusion of the encapsulated drug (sodium diclofenac) [37]. Thus, addition of TLL into the aqueous core of the insulin-loaded H_{II} mesophase could enable control of the insulin release rate. This would assist in the development of a novel insulin-carrier that could fully digest and release all the entrapped insulin. Additionally, since lipases perform an essential role in digestion by the GIT, examination of the insulin-loaded H_{II} system in the presence of TLL can emulate the GIT.

In the present study we aimed to design a smart biological carrier for insulin that would enable an efficient and sustained and controlled delivery. Insulin release would be examined in two aspects: (1) upon addition of TLL into the aqueous environment, and (2) upon addition of TLL directly into the insulin-loaded H_{II} mesophase. Additionally, the relationship between insulin release and the breakage of H_{II} structure was explored.

2. Experimental

2.1. Materials

Monoolein, distilled glycerol monooleate (GMO) (min. 97 wt% monoglycerides, 2.5 wt% diglycerides, and 0.4 wt% free glycerol; acid value 1.2, iodine value 68.0, and melting point 37.5 °C) was obtained from Riken Vitamin Co. (Tokyo, Japan). Phosphatidylcholine (PC) of soybean origin (Epikuron 200, min. 92 wt% PC) was purchased from Degussa (Hamburg, Germany). Tricaprylin (triacylglycerol, TAG) (97–98 wt%), *Thermomyces lanuginosa* lipase (TLL; 100,000 U/g), phosphate buffered saline (PBS; 0.01 M; pH 7.4), and dichloromethane were purchased from Sigma Chemical Co. (St. Louis, MO, USA). NovoRapid (insulin aspart; 100 U/mL solution for injection) was purchased from Novo Nordisk (Bagsvaerd, Denmark). The water was double distilled. All components were used without further purification.

2.2. Preparation of H_{II} mesophases

Four reverse hexagonal liquid crystal systems composed of GMO/TAG/(insulin solution), GMO/PC/TAG/(insulin solution), GMO/TAG/(insulin solution)/TLL, and GMO/PC/TAG/(insulin solution)/TLL with weight ratios of 72/8/20, 63/10/7/20, 71.1/7.9/20/1, and 62.1/10/6.9/20/1, respectively, were prepared. In order to study the influence of PC and TLL on the mesophases, they were solubilized at constant concentrations while decreasing the GMO and TAG concentrations but keeping the weight ratio of GMO/TAG (9:1) and insulin solution (NovoRapid) content of 20 wt% constant. The weighed quantities of GMO, TAG, and PC were mixed while heating to 80 °C. The samples were stirred and cooled to 32 °C. An appropriate quantity of the insulin solution and TLL were added and the samples were stirred. Additionally, 1000 U/g TLL solution in PBS was prepared.

2.3. Insulin release kinetics

A vertical Franz diffusion cell (PermeGear, Inc., Hellertown, PA, USA) was used to determine the insulin release profile of the various formulations. The receptor chamber was filled with 5 mL PBS (pH 7.4) with or without 1000 U/g TLL. Then, freshly prepared liquid crystal formulations were mounted on a supporting membrane (100 μm; Millipore, Bedford, MA, USA) and clamped over the filled receptor (diffusion area 0.64 cm^2). The apparatus was constantly stirred (500 rpm) and kept at 32 ± 0.5 °C. At 0.5, 1, 3, 5, and 8 h, 0.4 mL samples were taken from the receptor chamber, and insulin content was measured twice by enzyme-linked immunosorbent assay (ELISA) (Mercodia, Sweden). Each sampling was followed by insertion of 0.4 mL of fresh PBS or 1000 U/g TLL solution in PBS. The experiment was repeated three times.

2.4. Cross-polarized light microscope

Microscopic observations were performed using a Nikon model Eclipse 80i microscope equipped with Digital camera model DXM 1200C (Nikon, Tokyo, Japan). The samples were inserted between two glass microscope slides and observed with cross-polarizers.

2.5. Lipolysis kinetics

Lipolysis of the H_{II} mesophases was monitored by breakage of the H_{II} structures at various time points. Fifty mg of the appropriate insulin-loaded H_{II} system were inserted in a test tube with 0.2 mL PBS with or without 1000 U/g TLL, for different time periods. 5 mL of dichloromethane were added to each test tube, and stirred to complete breakage of the H_{II} structure and phase separation. A sample was then immediately collected from the dichloromethane phase (to avoid further lipolysis). The samples were injected into the GCMS for analysis of the lipid composition.

2.6. Gas chromatography–mass spectroscopy (GC–MS)

Chromatographic measurements were performed using GC–MS with 7890A GC and 5975C MSD detector (Agilent Technologies, Santa Clara, CA, USA). The ionization source was of an electron ionization (EI) mode. Solution was injected into a DB-5MS capillary fused silica column (0.25 mm diameter, 15 m length, 0.25 μm internal coating) (Agilent Technologies). Injector temperature was set to 290 °C. The column temperature was measured from 60 °C to 290 °C at 25 °C/min. Regression and statistical analysis of the obtained data were conducted using the GC–MS ChemStation software package and NIST library.

3. Results

3.1. Enzymatic lipolysis of the insulin-loaded H_{II} mesophase

The stability of the insulin-loaded H_{II} structures, with and without PC, was studied by addition of TLL to the environment of the H_{II} systems or into the core of the H_{II} structures. The TLL that was placed in the aqueous environment is mimicking the situation in our guts. We termed this TLL, in short, the "outer TLL". While by adding the TLL in the aqueous channels together with the insulin its effect was more localized and we hoped to obtain better control of insulin release. We termed this TLL, in short the "inner TLL". When

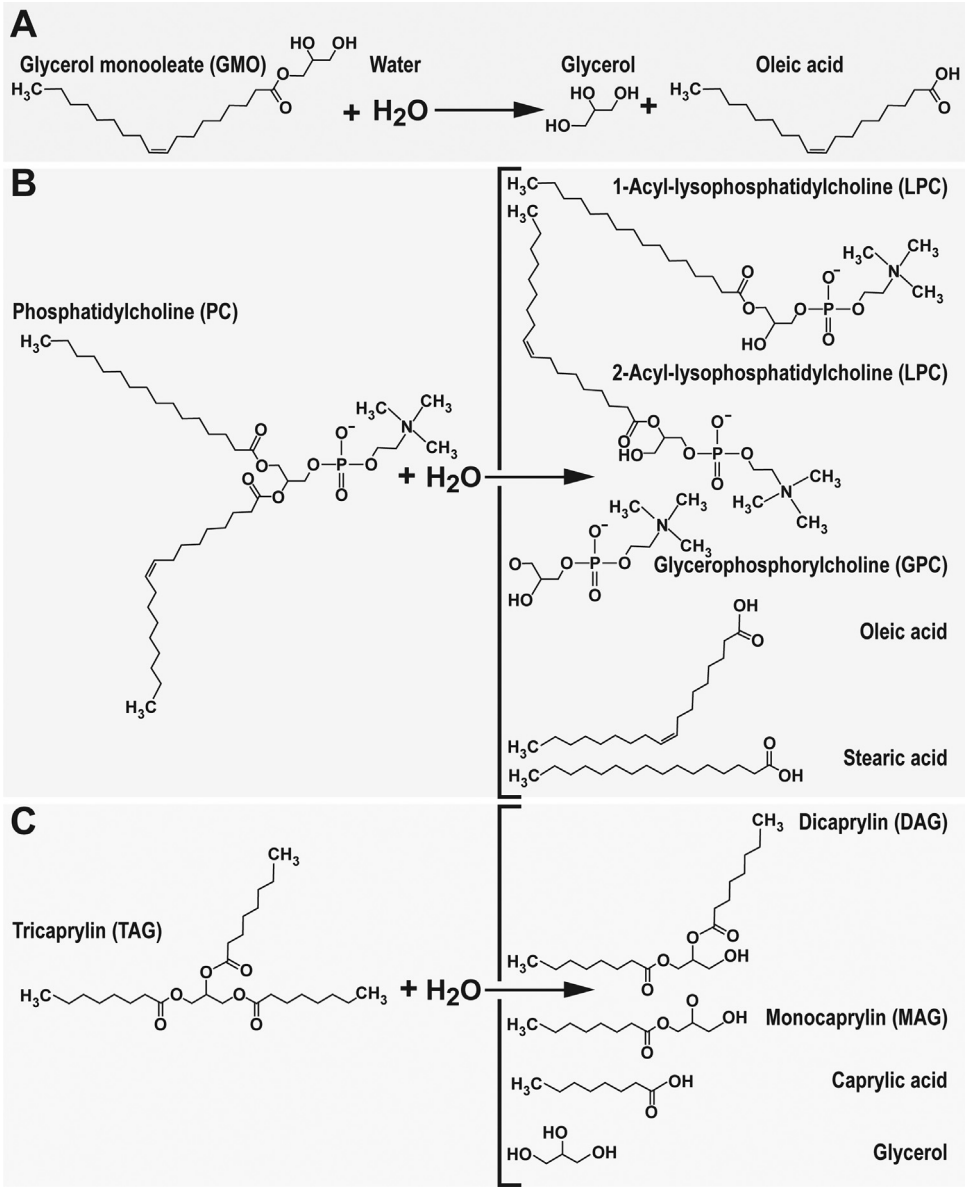

Fig. 1. Schematic presentation of TLL enzymatic hydrolysis of: (A) glycerol monooleate (GMO), (B) phosphatidylcholine (PC), and (C) tricaprylin (TAG).

no TLL was present, the insulin-loaded H_{II} carriers maintained their hexagonal symmetry in the presence and in the absence of PC.

However, when (outer or inner) TLL was added to the system, enzymatic lipolysis of GMO, PC and TAG took place, resulting in destruction of the H_{II} structure. Fig. 1A–C presents the lipolysis processes of the GMO, PC, and TAG, and the formation of the corresponding fatty acids.

Each system was followed up to full destruction of the H_{II} symmetry by cross-polarizing light microscope. Fig. 2A–F illustrates the microscope images of the different H_{II} structures, 8 h after preparation.

The times required for a full decomposition of the H_{II} structures were determined visually by transition of all the gel formulation into a solution. These, together with the confirmation of their decomposition by microscope images (Fig. 2A–F), could demonstrate that there are significant differences in the decomposition kinetics as a function of TLL location.

When TLL was embedded (solubilized) within the aqueous core of the H_{II} channels, the H_{II} structure decomposed ~6 times faster than when TLL was in the aqueous environment (the time elapsed until full decomposition of the H_{II} structure was 5 h in the inner TLL system and 30 h in the outer TLL system, in the absence of PC, and 18 h in the inner TLL system and 100 h in the outer TLL system, in the presence of PC; Table 1). The microscope images (Fig. 2C vs. E, and Fig. 2D vs. F) also illustrate that TLL embedment within the H_{II} channels resulted in much rapid decomposition of the structures than if it was present in the outer environment. These differences can be explained by at least three factors: (1) inner TLL had more interactions (higher local concentration) with the lipid molecules than

Table 1
Time (hr) elapsed until full decomposition of the H_{II} structure.

	Time (h)	
	Without PC	With PC
No TLL	stable	stable
Outer TLL	30	100
Inner TLL	5	18

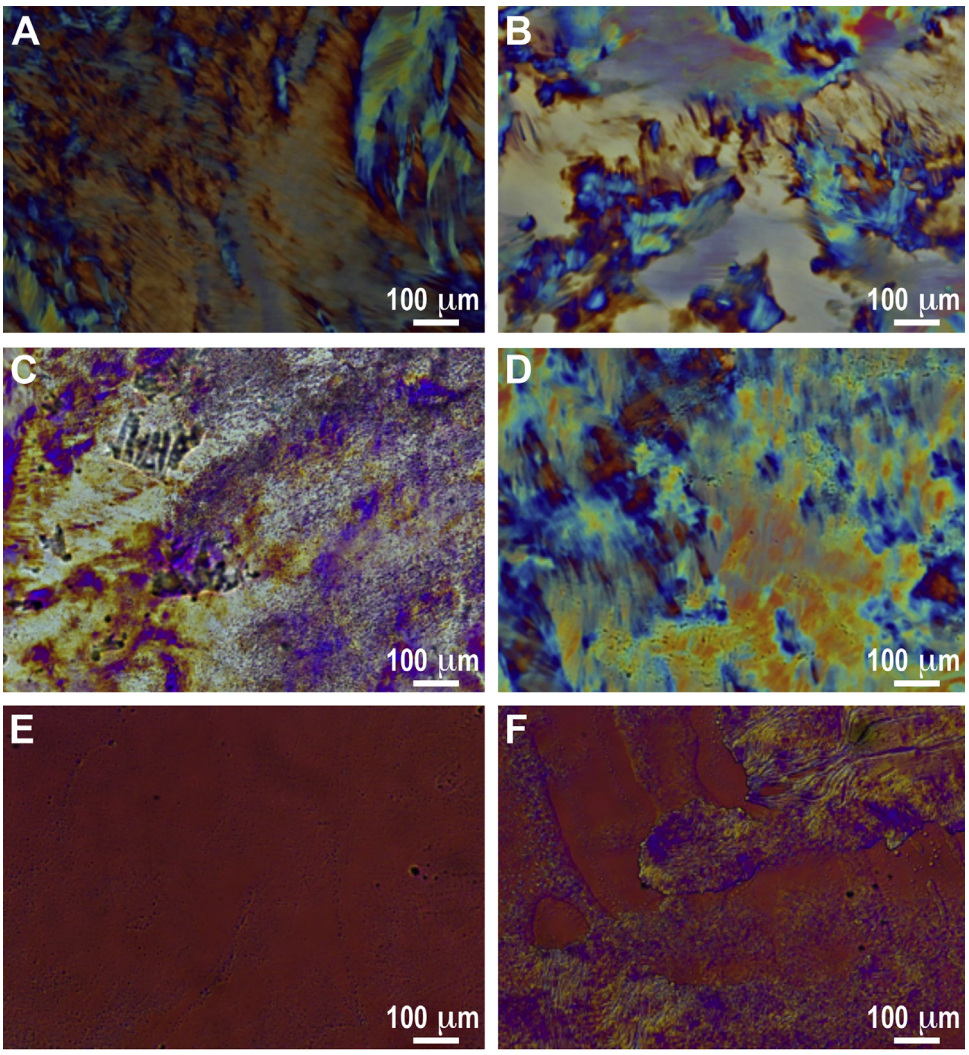

Fig. 2. Cross-polarizing light microscopy images of H_{II} system containing: (A) GMO/TAG/(insulin solution), (B) GMO/PC/TAG/(insulin solution), (C) GMO/TAG/(insulin solution) in TLL environment (D) GMO/PC/TAG/(insulin solution) in TLL environment, (E) GMO/TAG/(insulin solution)/TLL, and (F) GMO/PC/TAG/(insulin solution)/TLL, 8 h after preparation.

outer TLL that interacted only with the carboxylic groups somewhat hidden in the aqueous channels, (2) the active site of the inner TLL was closer and in good contact with the carboxylic groups (the substrate) attacking them more efficiently than the outer TLL, and (3) the active site of the TLL, which exists in two forms, closed (inactive) and open (active) [38], can be modified upon encapsulation [39].

The mesophases were constructed and exposed to TLL once without PC and once in its presence. The aim was to understand the role of PC along with the TLL on the control of the insulin release in the presence of the TLL.

Composing the H_{II} mesophases with PC hindered the destruction process of the H_{II} structure ~3.5 times slower than in the absence of PC (the time elapsed until full decomposition of the H_{II} structure was 30 h in the absence of PC and 100 h in the presence of PC in the outer TLL system, and 5 h in the absence of PC and 18 h in the presence of PC in the outer TLL system; Table 1). PC is structure builder and kosmotropic agent to the H_{II} mesophase increasing its stability. The microscope images (Fig. 2C vs. D, and Fig. 2E vs. F) illustrate the PC effect on the decomposition kinetics. It is clear that the addition of PC has a strong stabilization effect on the H_{II} structure, forming a more compact and more tightly packed interface [31,40], resulting in more hindered contact of the enzyme to the active site. The effect indeed inhibited the lipolysis process.

The stability of the H_{II} structure was expressed by the hydrolysis of the TAG and the formation of the lipolysis products was studied (Fig. 1A–C). We intentionally destructed the H_{II} structures and explored the lipolysis products at different time intervals. The content of GMO and TAG, and their hydrolysis products (oleic acid and DAG, respectively; Fig. 1A and C), up to a complete structure destruction, were quantified using GC–MS. The molar concentration of each component was calculated from the peaks' areas, and was plotted against time (Fig. 3A–D). Since oleic acid is also a metabolite of PC (Fig. 1B), in the GMO/TAG/PC-based systems, the measured molar concentration of the oleic acid could be up to 15 mol% bigger than the real concentration.

It should be noted that no lipolysis products were detected in the absence of TLL, and no noticeable differences were detected between the chromatograms of the two H_{II} systems (with and without PC) (data not shown).

As expected, addition of outer TLL gradually increased the molar fraction (expressed in mole percentage) of the hydrolysis products as a function of time (Fig. 3A and B). In the presence of PC, the progress in the hydrolysis process and production of the

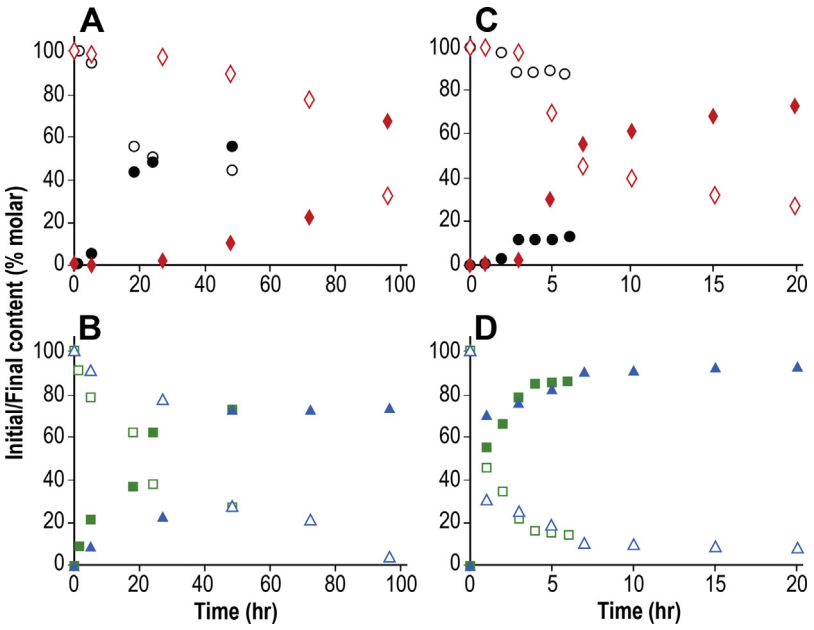

Fig. 3. Lipolysis kinetics of the H_{II} systems ((A) and (B)) when TLL is in the environment, and ((C) and (D)) when TLL is embedded within the cylinders. (●) oleic acid, (○) GMO, (■) DAG, and (□) TAG in the GMO/TAG-based H_{II} mesophase composed. (♦) oleic acid, (◊) GMO, (▲) DAG, and (△) TAG in the GMO/PC/TAG-based H_{II} mesophase.

metabolites were moderate, pointing again to the stabilization of the structure, which hindered the lipolysis process. The impact of the lipolysis on the two H_{II} systems was also compared, at the time frame, in which the H_{II} structures were completely destructed (after 30 and 100 h in the absence and in the presence of PC, respectively). At these time points, even though it seemed that the H_{II} structure was decomposed, only 50 mol% of GMO was hydrolyzed to form oleic acid in the absence of PC, while 70 mol% of GMO was hydrolyzed to form oleic acid in the presence of PC. Additionally, only 65 mol% of TAG was hydrolyzed to form DAG in the absence of PC, while 75 mol% of TAG was hydrolyzed to form DAG in the presence of PC. Hence, more pronounced lipolysis should take place in order to completely destruct the H_{II} structure containing PC.

Embedment of TLL within the H_{II} channels (inner TLL) gradually increased the molar percent of the hydrolysis products as a function of time (Fig. 3C and D). Analysis of the molar concentration of the hydrolysis products, with and without PC, revealed only minor differences. This is in contrast to the lipolysis rate that was detected when TLL was in the system's environment (outer TLL). Hence, it is assumed that when TLL was located in the system's environment, it first interacted with TAGs and the lipids' tails, leading to more dominant TAG lipolysis. Since the active site of the TLL was far from the lipids-water interface, its activity was hindered [41]. With time, TLL succeeded to penetrate the interface "from in out", resulting in lipolysis of the GMO. However, since the addition of PC stabilized the interface, it more efficiently blocked the access of TLL to the GMO ester groups.

The lipolysis rate of the H_{II} systems containing TLL was compared at the time intervals in which the H_{II} structures were completely destructed (after 5 and 18 h in the absence and in the presence of PC, respectively). At these time points, even though it seemed that the H_{II} structure was decomposed, only 10 mol% of GMO was hydrolyzed to form oleic acid in the absence of PC, while 70 mol% of GMO was hydrolyzed to form oleic acid in the presence of PC. Additionally, only 85 mol% of TAG was hydrolyzed to form DAG in the absence of PC, while 95 mol% of TAG was hydrolyzed to form DAG in the presence of PC. These results demonstrate again that more pronounced lipolysis is needed in order to break the GMO/PC/TAG-based structure.

3.2. The impact of TLL on insulin release from the H_{II} mesophase

The kinetic release profile of insulin from the liquid crystal was investigated by the Franz cell apparatus. This experimental platform is based on a physical separation of the colloidal nanostructures from the receptor chamber by an artificial membrane, from which samples were withdrawn to quantify insulin content. Several previous studies on liquid crystal-based release system used this approach [42–44]. Thus, lower aggregates and non-dissolved particles are expected in comparison to the USP dissolution apparatus (bath). In addition, the lower volume used in the Franz cell system may increase the sensitivity of the system. On the other hand, it should be noted that this non-automated method requires extensive training to generate reproducible results.

Cumulative release of insulin from the H_{II} mesophase was monitored as a function of PC and TLL, and was plotted as time-dependent release (Fig. 4A–C). In the absence of TLL, release was very slow (as expected from H_{II} mesophase). In both cases most of the release occurred in the first three hours (Fig. 4A). Yet, the H_{II} systems demonstrated different release kinetics with or without PC. Addition of PC drastically increased insulin release rate (11% insulin was released in the presence of PC while only 2% insulin was released in the absence of PC, after 3 h). After the first three hours, a strong drop in insulin cumulative release was detected in the absence of PC, from 2% after 3 h to only 1% after 5 h. Similarly but in less extend, in the presence of PC the commutative release dropped from 11% after 3 h to only 5% after 5 h. Since it is not likely that insulin diffused out of the receptor compartment, the explanation for this effect might be related to the fact that after five hours we are no longer detecting (recording) the insulin that released. After 5 h, a major fraction of the released insulin molecules, were no longer stable in the PBS solution, as insulin has a poor stability in aqueous solution and a strong tendency to aggregate [45]. Therefore, the actual percentage of insulin released is probably higher than the measured. After eight hours, a further decrease in insulin release was not detected although insulin was even less stable in the PBS solution (Fig. 4A); thus, insulin had to continue to release from the H_{II} system.

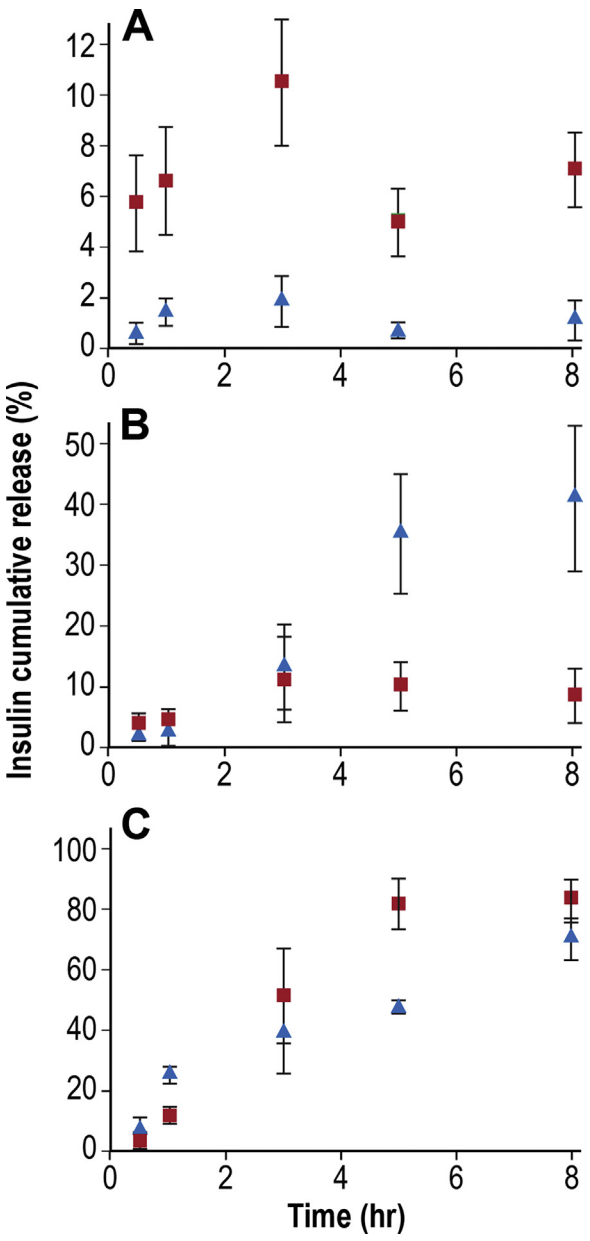

Fig. 4. Insulin cumulative release from the (▲) GMO/TAG-based H_{II} system and (■) GMO/PC/TAG-based H_{II} system: (A) with no TLL, (B) to TLL environment, and (C) when TLL is embedded within the H_{II} cylinders.

These release measurements are in agreement with our previous published results, in which the release of human recombinant insulin from the H_{II} system was monitored [31]. It was shown that most of the release occurred in the first 40 min, followed by a more moderate release. In the present study, the release was slower, since an artificial membrane was used. Hence, it created a barrier (obstruction) that extended the first stage of the release, in which the diffusion process of insulin was dominant. The moderate release of insulin, which was detected in the second stage of release, was explained by a resistance process that significantly slowed it down. This resistance process (denoted as obstruction factor) was attributed to the blockage of the lipid membrane by insulin. Once insulin diffusion started, it was transported through the lipid layer and "set" in it, hindering further diffusion.

The addition of PC increased insulin release as was already detected and investigated [31]. PC increased the spacing between the tails, providing more mobility to the cylinders. As a result, a more cooperative system was formed, meaning that the movements of the lipophilic tails indirectly induce fluctuations in the GMO heads, as detected by dielectric spectroscopy [46] and rheological analysis using Bohlin model [31].

Addition of TLL to the H_{II} mesophase environments (outer TLL) revealed different behaviors (Fig. 4B). In the absence of PC, insulin release gradually increased as a function of time until it reached 41% after 8 h. Since insulin has poor stability in aqueous solution [45], the actual release is probably much higher. The release, based on decomposition rate of the insulin led to estimate its release to be of ca ~43% after 5 h, and more than 50% after 8 h. Hence, the presence of TLL in the outer environment of this system had very strong effect on the insulin release. The major impact of the TLL could already be observed after 3 h, in which 13% of the insulin was released compared to only 2% in the absence of TLL. Therefore, we concluded that the contact of the H_{II} system with the TLL, even if it comes from an outer environment (for example, the guts) disordered and destructed the hexagonal mesophase and enhanced the insulin release.

The presence of PC in the H_{II} system showed a very surprising behavior, as the release was similar to that in the absence of TLL. These results indicate that the structure did not modify in the first 8 h, as PC stabilized the interface and hindered the lipolysis. This is also supported by the microscope image of the system (Fig. 2D) and by the GC–MS analysis, after 8 h (Fig. 3A and B). Once sufficient amount of the GMO and TAG were hydrolyzed the release of the insulin increased significantly (data not shown).

Insulin release from the TLL-loaded in the aqueous phase of the H_{II} mesophases (inner TLL) demonstrated dramatic increase in its release as a function of time (Fig. 4C). In the absence of PC, insulin release gradually increased as a function of time until it reached 48% after 5 h. Since insulin has poor stability in aqueous solution [45], the actual release was calculated (an estimated) using the measurements of the reference system without TLL. The actual calculated insulin release reached 80% after 5 h, and up to 100% after 8 h.

Upon addition of PC, a unique behavior was recorded. During the first hour, insulin release was lower in the presence of PC than the release in its absence, but after 5 h the measured release reached 85%, pointing to actual release of up to 100%. Hence, it is assumed that during the first hour PC inhibited the lipolysis process. Therefore the structure was less damaged and insulin diffused more slowly. However, when the structures started to crack, PC enhanced insulin release as was detected after 5 h.

In the present manuscript we had focused only on the reverse hexagonal liquid crystalline phase (H_{II} mesophases), and not on their dispersions (hexosomes). It is possible to prepare hexosomes based on our H_{II} carriers (GMO/TAG/water system), however the problem of using such dispersions is that the solubilized drug is released into the aqueous medium before it is given to the patient (on the shelf). Another disadvantage is the limited capacity of the solubilized drug.

4. Conclusions

The addition of TLL to the environment of the H_{II} systems (outer TLL) resulted in lipolysis and destruction of the H_{II} structures, as monitored by cross-polarized light microscope and by the increase in the molar concentration of the lipolysis products (GC–MS analysis). In the absence of PC, the TLL lipolysis effect was more dominant and led to a significant increase in insulin release (50% after 8 h). However, when PC was added to the H_{II} system, the interface was better stabilized. As a result, the lipolysis process was hindered, and no impact on the release profile was detected in the first 8 h.

Entrapment of TLL within the H_{II} cylinders (inner TLL) drastically enhanced the destruction of the H_{II} structures as monitored

by microscope images and GC–MS analysis. As a result, all the entrapped insulin was released from the system (100% after 5–8 h). Analysis of the molar concentration of the hydrolysis products with and without PC revealed only minor differences in the first hours. Yet, more lipolysis was needed in order to fully destruct the H_{II} symmetry.

In conclusion, this study demonstrates that insulin release from the H_{II} carriers can be controlled by the addition of PC and in the presence of lipases. Lipase enhanced both the destruction of the carrier and the release of the entrapped drug. PC hindered the lipolysis and therefore slowed insulin release. The controlled release could improve glucose control in the treatment of diabetic patients. This study can be used for a future design of insulin release from lyotropic liquid crystals.

Acknowledgments

The study was supported by grants from the ICA Foundation and the Israel Ministry of Science, Technology and Space.

References

[1] J.P. Hill, L.K. Shrestha, S. Ishihara, Q. Ji, K. Ariga, Self-assembly: from amphiphiles to chromophores and beyond, Molecules 19 (2014) 8589–8609.
[2] J.M. Seddon, Structure of the inverted hexagonal (HII) phase, and non-lamellar phase transitions of lipids, Biochem. Biophys. Acta 1031 (1990) 1–69.
[3] G.J.T. Tiddy, Surfactant-water liquid crystal phases, Phys. Rep. 57 (1980) 1–46.
[4] S. Milak, A. Zimmer, Glycerol monooleate liquid crystalline phases used in drug delivery systems, Int. J. Pharm. 478 (2015) 569–587.
[5] D. Libster, A. Aserin, N. Garti, Interactions of biomacromolecules with reverse hexagonal liquid crystals: drug delivery and crystallization applications, J. Colloid Interface Sci. 356 (2011) 375–386.
[6] F.S. Poletto, F.S. Lima, D. Lundberg, T. Nylander, W. Loh, Tailoring the internal structure of liquid crystalline nanoparticles responsive to fungal lipases: a potential platform for sustained drug release, Colloids Surf. B 147 (2016) 210–216.
[7] A.L.M. Ruela, F.C. Carvalho, G.R. Pereira, Exploring the phase behavior of monoolein/oleic acid/water systems for enhanced donezepil administration for Alzheimer disease treatment, J. Pharm. Sci. 105 (2016) 71–77.
[8] I. Amar-Yuli, D. Libster, A. Aserin, N. Garti, Solubilization of food bioactives within lyotropic liquid crystalline mesophases, Curr. Opin. Colloid Interface Sci. 14 (2009) 21–32.
[9] L. Sagalowicz, S. Guillot, S. Acquistapace, B. Schmitt, M. Maurer, A. Yaghmur, L. de Campo, M. Rouvet, M. Leser, O. Glatter, Influence of vitamin E acetate and other lipids on the phase behavior of mesophases based on unsaturated monoglycerides, Langmuir 29 (2013) 8222–8232.
[10] D. Libster, A. Aserin, I. Amar-Yuli, T. Mishraki, N. Garti, Crystallization of cyclosporine A in lyotropic reverse hexagonal liquid crystals, CrystEngComm 12 (2010) 2034–2036.
[11] A. Zabara, I. Amar-Yuli, R. Mezzenga, Tuning in-meso-crystallized lysozyme polymorphism by lyotropic liquid crystal symmetry, Langmuir 27 (2011) 6418–6425.
[12] A. Zabara, R. Mezzenga, Plenty of room to crystallize: swollen lipidic mesophases for improved and controlled in-meso protein crystallization, Soft Matter 8 (2012) 6535–6541.
[13] A. Zabara, R. Mezzenga, Modulating the crystal size and morphology of in meso-crystallized lysozyme by precisely controlling the water channel size of the hosting mesophase, Soft Matter 9 (2013) 1010–1014.
[14] L.S. Manni, A. Zabara, Y.M. Osornio, J. Schoppe, A. Batyuk, A. Pluckthun, J.S. Siegel, R. Mezzenga, E.M. Landau, Phase behavior of a designed cyclopropyl analogue of monoolein: implications for low-temperature membrane protein crystallization, Angew. Chem. Int. Ed. Engl. 54 (2015) 1027–1031.
[15] H. Qiu, M. Caffrey, The phase diagram of the monoolein/water system: metastability and equilibrium aspects, Biomaterials 21 (2000) 223–234.
[16] I. Amar-Yuli, N. Garti, Transitions induced by solubilized fat into reverse hexagonal mesophases, Colloids Surf. B 43 (2005) 72–82.
[17] C. Guo, J. Wang, F. Cao, R.J. Lee, G. Zhai, Lyotropic liquid crystal systems in drug delivery, Drug Discov. Today 15 (2010) 1032–1040.
[18] T. Mishraki, D. Libster, A. Aserin, N. Garti, Lysozyme entrapped within reverse hexagonal mesophases: physical properties and structural behavior, Colloids Surf. B 75 (2010) 47–56.
[19] T. Mishraki, D. Libster, A. Aserin, N. Garti, Temperature-dependent behavior of lysozyme within the reverse hexagonal mesophases (HII), Colloids Surf. B 75 (2010) 391–397.
[20] D. Libster, A. Aserin, D. Yariv, G. Shoham, N. Garti, Concentration- and temperature-induced effects of incorporated desmopressin on the properties of reverse hexagonal mesophase, J. Phys. Chem. B 113 (2009) 6336–6346.
[21] L. van t'Hag, S.L. Gras, C.E. Conn, C.J. Drummond, Lyotropic liquid crystal engineering moving beyond binary compositional space—ordered nanostructured amphiphile self-assembly materials by design, Chem. Soc. Rev. 46 (2017) 2705–2731.
[22] X. Liang, Y.L. Chen, X.J. Jiang, S.M. Wang, J.W. Zhang, S.Y. Gui, HII mesophase as a drug delivery system for topical application of methyl salicylate, Eur. J. Pharm. Sci. 100 (2017) 155–162.
[23] Y. Seino, K. Nanjo, N. Tajima, T. Kadowaki, A. Kashiwagi, E. Araki, C. Ito, N. Inagaki, Y. Iwamoto, M. Kasuga, T. Hanafusa, M. Haneda, K. Ueki, Report of the committee on the classification and diagnostic criteria of diabetes mellitus, J. Diabetes Invest. 1 (2010) 212–228.
[24] C.K. Kramer, B. Zinman, R. Retnakaran, Short-term intensive insulin therapy in type 2 diabetes mellitus: a systematic review and meta-analysis, Lancet Diabetes Endocrinol. 1 (2013) 28–34.
[25] P.V. Jayakrishnapillai, S.V. Nair, K. Kamalasanan, Current trend in drug delivery considerations for subcutaneous insulin depots to treat diabetes, Colloids Surf. B 153 (2017) 123–131.
[26] R.I. Henkin, Inhaled insulin-intrapulmonary, intranasal, and other routes of administration: mechanisms of action, Nutrition 26 (2010) 33–39.
[27] S. Soares, A. Costa, B. Sarmeneto, Novel non-invasive methods of insulin delivery, Expert Opin. Drug Deliv. 9 (2012) 1539–1558.
[28] T. Mishraki, M.F. Ottaviani, A.I. Shames, A. Aserin, N. Garti, Structural effects of insulin-loading into HII mesophases monitored by electron paramagnetic resonance (EPR) small angle X-ray spectroscopy (SAXS), and attenuated total reflection Fourier transform spectroscopy (ATR-FTIR), J. Phys. Chem. B 115 (2011) 8054–8062.
[29] T. Mishraki-Berkowitz, P. Ben Ishai, A. Aserin, Y. Feldman, N. Garti, The dielectric study of insulin-loaded reverse hexagonal (HII) liquid crystals, Phys. Chem. Chem. Phys. 17 (2015) 9499–9508.
[30] I. Amar-Yuli, D. Azulay, T. Mishraki, A. Aserin, N. Garti, The role of glycerol and phosphatidylcholine in solubilizing and enhancing insulin stability in reverse hexagonal mesophases, J. Colloid Interface Sci. 364 (2011) 379–387.
[31] T. Mishraki-Berkowitz, A. Aserin, N. Garti, Structural properties and release of insulin-loaded reverse hexagonal (HII) liquid crystalline mesophase, J. Colloid Interface Sci. 486 (2017) 184–193.
[32] V. Akbari, F. Hendijani, A. Feizi, J. Varshosaz, Z. Fakhari, S. Morshedi, S.A. Mostafavi, Efficacy and safety of oral insulin compared to subcutaneous insulin: a systematic review and meta-analysis, J. Endocrinol. Invest. 39 (2016) 215–225.
[33] S.G. Ramaswamy, V.G. Nayak, S.K. Jha, V. Hegde, V.S. Waichale, R. Melarkode, N. Chirmule, A.U. Rao, N. Sengupta, Development and validation of an electrochemiluminescent ELISA for quantitation of oral insulin tregopil in diabetes mellitus serum, Bioanalysis 9 (2017) 975–986.
[34] J. Borné, T. Nylander, A. Khan, Effect of lipase on different lipid liquid crystalline phases formed by oleic acid based acylglycerols in aqueous systems, Langmuir 18 (2002) 8972–8981.
[35] J. Borné, T. Nylander, A. Khan, Effect of lipase on monoolein-based cubic phase dispersion (cubosomes) and vesicles, J. Phys. Chem. B 106 (2002) 10492–10500.
[36] M. Marciello, C. Mateo, J.M. Guisan, Full enzymatic hydrolysis of commercial sucrose laurate by immobilized-stabilized derivatives of lipase from Thermomyces lanuginosa, Colloids Surf. B 84 (2011) 556–560.
[37] N. Garti, G. Hoshen, A. Aserin, Lipolysis and structure controlled drug release from reversed hexagonal mesophase, Colloids Surf. B 94 (2012) 36–43.
[38] N. Miled, A. de Caro, J. de Caro, R. Verger, A conformational transition between an open and closed form of human pancreatic lipase revealed by a monoclonal antibody, Biochim. Biophys. Acta 1476 (2000) 165–172.
[39] L. Nini, L. Sarda, L.C. Comeau, E. Boitard, J.P. Dube, H. Chahinian, Lipase-catalysed hydrolysis of short-chain substrates in solution and in emulsion: a kinetic study, Biochim. Biophys. Acta 1534 (2001) 34–44.
[40] D. Libster, P. Ben Ishai, A. Aserin, G. Shoham, N. Garti, Molecular interactions in reverse hexagonal mesophase in the presence of cyclosporin A, Int. J. Pharm. 367 (2009) 115–126.
[41] S. Santini, J.M. Crowet, A. Thomas, M. Paquot, M. Vandenbol, P. Thonart, J.P. Wathelet, C. Blecker, G. Lognay, R. Brasseur, L. Lins, B. Charloteaux, Study of Thermomyces lanuginosa lipase in the presence of tributyrylglycerol and water, Biophys. J. 96 (2009) 4814–4825.
[42] M.K. Kang, Y. Kim, S. Gil, S. Lee, J. Jang, S.J. Kim, M.S. Yoon, K.J. Yoo, J.B. Lee, H.S. Yoo, Effects of liquid crystal-based formulation on transdermal delivery of retinyl palmitate and proliferation of epidermal cells, Macromol. Res. 24 (2016) 44–50.
[43] E. Esposito, M. Drechsler, P. Mariani, A.M. Panico, V. Cardile, L. Crasci, F. Carducci, A.C.E. Graziano, R. Cortesi, C. Puglia, Nanostructured lipid dispersions for topical administration of crocin, a potent antioxidant from saffron (Crocus sativus L.), Mater. Sci. Eng. C: Mater. Biol. Appl. 71 (2017) 669–677.
[44] R. Cortesi, E. Cappellozza, M. Drechsler, C. Contado, A. Baldisserotto, P. Mariani, F. Carducci, A. Pecorelli, E. Esposito, G. Valacchi, Monoolein aqueous dispersions as a delivery system for quercetin, Biomed. Microdevices 19 (2017), http://dx.doi.org/10.1007/s10544-017-0185-0.
[45] L. Nielsen, R. Khurana, A. Coats, S. Frokjaer, J. Brange, S. Vyas, V.N. Uversky, A.L. Fink, Effect of the environmental factors on the kinetics of insulin fibril formation: elucidation of the molecular mechanism, Biochemistry 40 (2001) 6036–6046.
[46] T. Mishraki, P. Ben Ishai, D. Babukh, A. Aserin, Y. Feldman, N. Garti, Modulation of physical properties of HII mesophases: a dielectric spectroscopy study, J. Colloid Interface Sci. 396 (2013) 178–186.